XXI IMEKO World Congress "Measurement in Research and Industry"
August 30 – September 4, 2015, Prague, Czech Republic

MEASUREMENTS OF INERTIAL ACOUSTIC CAVITATION EMISSIONS AND THEIR CORRELATION WITH EROSION RESISTANCE OF STAINLESS STEEL 304

I. Ibanez [1], *M. Hodnett* [2], *B. Zeqiri* [2], *M. N. Frota* [1]

[1] Postgraduate Programme in Metrology (PósMQI), Catholic University of Rio de Janeiro, RJ, Brazil, ivanez@aluno.puc-rio.br, mfrota@puc-rio.br
[2] Acoustics and Ionising Radiation Division, National Physical Laboratory (NPL), Hampton Road, Teddington, U.K., mark.hodnett@npl.co.uk, bajram.zeqiri@npl.co.uk

Abstract – This work describes a ASTM G32-10 compliant technique for measuring ultrasonic cavitation used to induce erosion in engineering materials. The hydrodynamic cavitation erosion resistance of coupons of stainless steel 304 was investigated by exposure of the material to acoustic cavitation generated by an ultrasound transducer. A 65 mm diameter variant of a cavitation sensor developed by the National Metrology Institute of the UK (NPL) proved to detect broadband acoustic emissions and logs acoustic signals produced in the MHz frequency range. The readings of cavitation were made during the exposure duration at discrete intervals (900 to 7200 s) enabling periodic mass measurements (evaluation of erosion) under a strict protocol. Cavitation measurements were carried out for different positions of the ultrasound transducer horn confronting the material exposed to erosion. For a transducer displacement amplitude of 43.5 µm, maximum variation in measurements of cavitation level was found to be between 2.6% and 3.8% when the separation (λ) between the transducer horn and the specimen amplified from 0.5 to 1.0 mm, respectively. Mass loss of the specimen —a measure of erosion— was 7.5 mg (λ=0.5 mm) and 6.8 mg (λ=1.0 mm) for experiments carried out at the same transducer displacement amplitude.

Keywords: Metrology, cavitation erosion, ultrasound, CaviMeter, stainless steel 304, standard ASTM G32-10.

1. INTRODUCTION

Stainless steel 304 is an extensively used engineering material often subject to cavitation erosion when submerged in fluids undergoing rapid reduction in pressure with respect to their correspondent saturation vapour pressure. Common examples of this kind of wear often happen in pump impellers, and bends where sudden changes in the direction of liquid may cause surface fatigue of the metal damaging its physical integrity. Different searches for solutions to understand the phenomenon and to reduce its detrimental effect have inspired research on the subject [1-5]. In particular, this paper describes part of a broader work [6] developed to evaluate the resistance to cavitation erosion induced in engineering materials. Due to space limitation, this paper focuses on the cavitation erosion in specimens of stainless steel 304. The study was developed according with well-established specification standards that describes an ASTM G32 compliant method for cavitation erosion [7].

The erosion process was based on measuring of mass loss of the specimen while measurements of cavitation were performed by a variant of the NPL's cavitation sensor (the CaviMeter) [8].

2. THEORETICAL BACKGROUND

2.1 Cavitation erosion

Generally, cavitation results from the formation of vapour cavities in a liquid. Under rarefaction condition, horseshoe vortices originated in the low-pressure fluid tend to concentrate the vorticity toward the material surface centrifuging out heavier liquid particles. This is a well-understood non-stable mechanism that breaks monolithic cavities into bubbles caused by the high fluid velocities [5].

The acoustic cavitation develops in two regimes: inertial and non-inertial [9]. The first occurs in the absence of bubble collapse (bubbles may increase or decrease in diameter in response to the driving ultrasonic field) [4] and the latter occurs with the eventual collapse of the bubbles. Figure 1 illustrates both regimes.

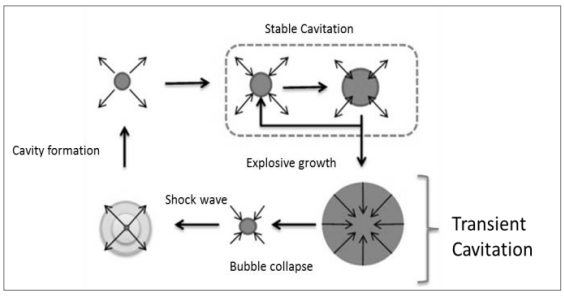

Fig.1. Cavitation sequence. Source: modified from [5]

According to standard ASTM G32: 2010, erosion develops in stages [7]:

- Incubation stage: erosion rate is insignificant at the beginning of the process;
- Acceleration stage: erosion rate rises until ranges a maximum value;
- Deceleration stage: erosion rate is reduced as a result of change in roughness at the eroded surface.

2.2 Calibration of the CaviMeter

A pioneering method to calibrate the CaviMeter was recently devised by NPL where the calibration of the

CaviSensor requires derivation of its sensitivity in terms of V/Pa. The calibration procedure (integrated over the range 1.5 - 7 MHz) uses a conventional hydrophone to characterise the acoustic pressure distribution at the distance corresponding to the position of the CaviSensor receiving element. With the CaviSensor connected to CaviMeter (at specific gain settings), keeping the cylindrical transducer co-aligned, the average RMS pressure values determined from beam plotting measurements is compared with displayed CaviMeter values, yielding a system sensitivity = 96.2 mV/Pa @ 2.45 MHz. Although this calibration procedure ensures a spatially-sensitive cavitation sensor that determines the average RMS acoustic pressures emitted by multi-bubble inertial cavitation it still denotes a 'first approximation' calibration, as it so far doesn't account for (i) the variation in the measured acoustic field over the conceptual cylinder; (ii) variation in the inherent CaviSensor film sensitivity over its surface and (iii) variation in the CaviSensor frequency response over the calibration range [10].

2.3 Measurements of cavitation

Figure 2 illustrates a variant of the cavitation sensor used for (quantitative) measurements of cavitation [8, 11] at frequencies above 20 kHz. The acoustic emission of bubbles is detected by a piezoelectric sensor (PVDF type, 52 microns of thick, coated with a special rubber to isolate it from the fluid medium) and the acoustic waves generated by an ultrasound transducer driven by an external power supply. Hodnett and Zeqiri [12] describe the acoustic cavitation meter developed at the National Physical Laboratory (NPL).

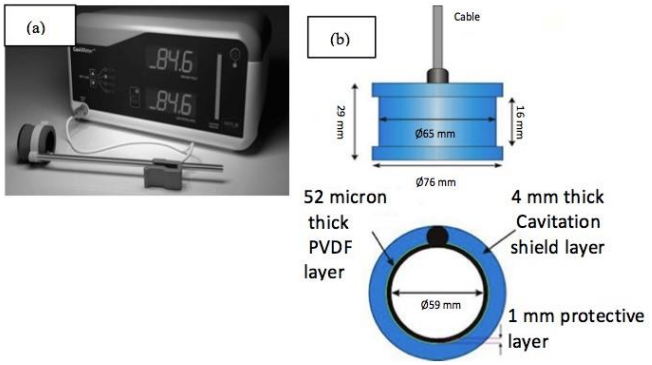

Fig. 2. (a) Cavimeter; (b) Cavitation sensor geometry

Two are the output signals of the CaviMeter:

- **Acoustic signal at the fundamental frequency** (operating frequency of the ultrasound transducer) that allows measurement of the so called driving field. The CaviMeter uses electronic filters in the broadband of 20-60 kHz in order to determine the acoustic signal and get the specific signal from the operating frequency of the transducer [1].
- **acoustic emission signal** created by bubble collapse, covering frequency components between 1.5 and 8 MHz, that allows measurement of the cavitation level. Measurement of the CaviMeter uses electronic filters in a specific broadband in order to isolate acoustic signals generated from bubble collapse [1].

Figure 3 decodes these outputs in terms of the signals:

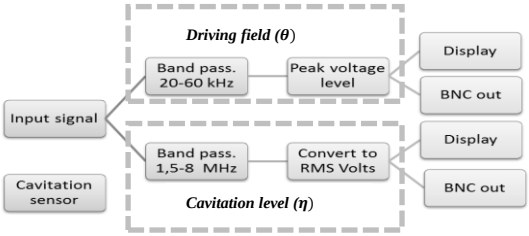

Fig. 3. Cavimeter output signals

3. EXPERIMENTAL PROCEDURE

The cavitation erosion process develops within a fluid media (distilled water at 22±2 C), where cavitation is induced by a 20 kHz ultrasonic transducer (Model 23820A, manufactured by Sonic Systems Ltd.). Table 1 characterizes properties of the stainless steel 304.

Table 1. Characteristics of the stainless steel 304

Specific mass (mg/mm^3)	Brinell Hardness (HB)	Dimensions (mm)
7.94	201	Ø25 X 5

According to the applicable standard (ASTM G32:2010), the cavitation erosion experiments were developed under specific operating conditions; i.e.: for two values of transducer-sample separation (λ) of the transducer horn with respect to the specimen, at a fixed value of the transducer amplitude (δ); i.e.:

- experiment #1: [δ = 43.5 μm; λ = 0.5 mm]
- experiment #2: [δ = 43.5 μm; λ = 1.0 mm]

The electrical power (59 W) of the drive unit (Sonic Systems, Processor P100/3-20) produces a transducer amplitude of 43.5 μm. Both experiments were developed in accordance with the schematic configuration illustrated in Figure 4.

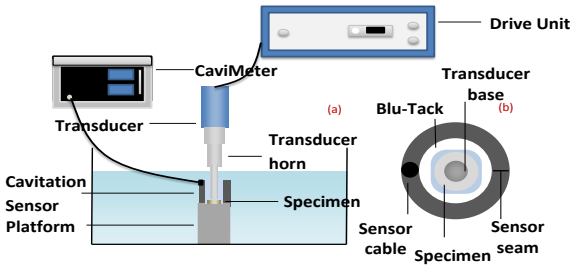

Fig. 4. Assembling of the cavitation erosion experiment

An electronic weighing scale (LP1200s series, manufactured by Sartorius, resolution of 1 mg) was used to weigh the specimens before and after their exposure to erosion.

4. EXPERIMENTAL RESULTS

Cavitation measurements (cavitation levels) were performed under a strict protocol during the time of exposure of the stainless steel 304 specimen to erosion (discrete intervals of time varying from 900 to 7200 s), allowing periodic mass measurements to assess erosion.

4.1 Analysis focused on the cavitation phenomena

Figure 5 and 6 illustrate measurements of the cavitation level (θ) associated with experiments #1 and #2, respectively, for each one of the discrete intervals studied.

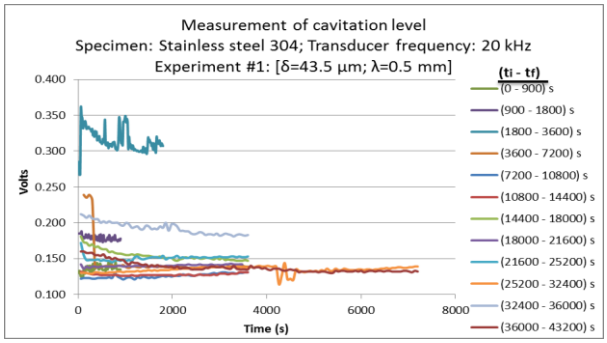

Fig. 5. Cavitation level for at experiment #1

For both experiments, measurements of cavitation were analysed through the statistical Chi-squared test (Equation), to evaluate whether or not cavitation follows a uniform pattern on each discrete interval.

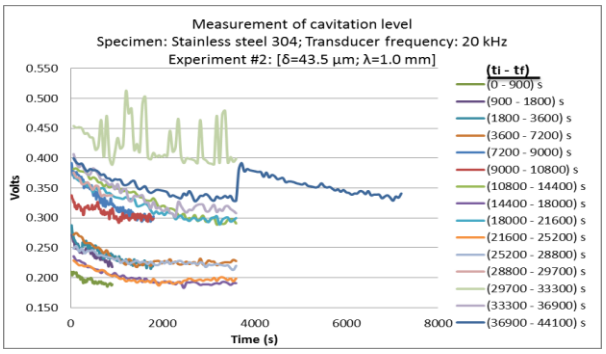

Fig. 6. Cavitation level for at experiment #2

$$Q = \sum \frac{(f_i - e_i)^2}{e_i}$$

In this equation, f_i is the real frequency of occurrence of the level of cavitation in a given time interval and e_i the associated theoretical frequency. For a confidence level of 99%, the cavitation level follows a uniform pattern if the tabulated value of the test (X^2) satisfy the condition: $X^2 > Q$.

Table 2 and 3 summarize, for each one of the discrete intervals ($t_f - t_i$), the statistical parameters (Q, X^2) that support the Chi-squared analysis. A statistical analysis that allows interpretation of the uniform or non-uniform character of the results, also yielding the average value of measurements of cavitation ($\bar{\theta}$); The statistical parameter (u_s) expresses the variation of measurement associated with the cavitation level.

Table. 2. Statistical analysis of experiment #1

Discrete intervals	$t_i\ (s)$	$t_f\ (s)$	$(t_f - t_i)$	N_m	Q	χ2	Uniform or non-uniform Pattern?	$\bar{\theta}\ (Volt)$	us (%)
1	0	900	900	60	34.6	15.09	No	0.196	1.3
2	900	1800	900	60	7.4	15.09	Yes	0.240	1.5
3	1800	3600	1800	30	28.28	16.81	No	0.238	1.9
4	3600	7200	3600	60	38.67	13.28	No	0.233	1.5
5	7200	9000	1800	30	32.55	20.1	No	0.327	1.3
6	9000	10800	1800	30	13	16.81	Yes	0.308	1.7
7	10800	14400	3600	60	13.74	16.81	Yes	0.328	1.0
8	14400	18000	3600	60	19.33	13.28	No	0.200	1.0
9	18000	21600	3600	60	13	15.09	Yes	0.320	1.1
10	21600	25200	3600	60	27.2	15.09	No	0.201	1.1
11	25200	28800	3600	60	29.33	13.28	No	0.229	1.1
12	28800	29700	900	60	2.33	11.34	Yes	0.352	1.1
13	29700	33300	3600	60	27.17	13.28	No	0.425	7.4*
14	33300	36900	3600	60	13.67	13.28	No	0.335	1.8
15	36900	44100	7200	120	14.67	18.48	Yes	0.353	3.1
			Total Number of measurements N_m	870					*Outlier

Table. 3. Statistical analysis of experiment #2

Discrete intervals	$t_i\ (s)$	$t_f\ (s)$	$(t_f - t_i)$	N_m	Q	χ2	Uniform or non-uniform Pattern?	$\bar{\theta}\ (Volt)$	us (%)
1	0	900	900	60	29.8	15.09	No	0.136	3.1
2	900	1800	900	60	13.71	15.09	Yes	0.182	1.6
4	3600	7200	3600	60	58.20	16.81	No	0.148	8.3*
5	7200	10800	3600	60	9.07	16.81	Yes	0.126	0.9
6	10800	14400	3600	60	33.8	13.28	No	0.128	0.4
7	14400	18000	3600	60	32.00	15.09	No	0.155	0.9
8	18000	21600	3600	60	3.71	11.34	Yes	0.142	0.6
9	21600	25200	3600	60	31.93	13.28	No	0.151	1.7
10	25200	32400	7200	120	12.47	11.34	No	0.135	2.6
11	32400	36000	3600	60	10.40	15.09	Yes	0.193	1.3
12	36000	43200	7200	120	148.83	21.70	No	0.138	1.1
			Total Number of measurements N_m	810					*Outlier

4.2 Analysis focused on the erosion phenomena

Results shown in Figures 7 and 8 confirm that the mass loss associated with experiment #1 (δm = 7.5 mg) is 6.2% higher than that of experiment #2 (δm = 6.8 mg). Furthermore, these figures illustrate the behaviour of the erosion rate associated with both experiments carried out at the discrete intervals investigated. As observed, the higher the erosion rate the higher the mass loss.

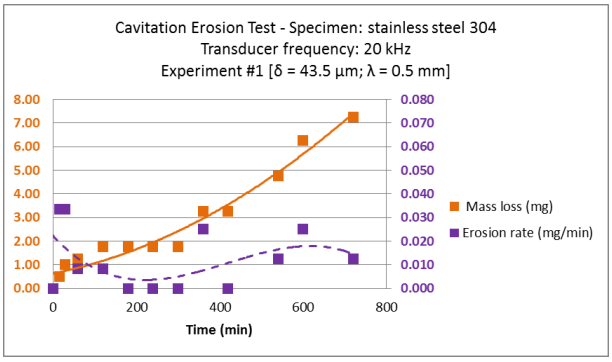

Fig. 7. Mass loss associated with experiment #1

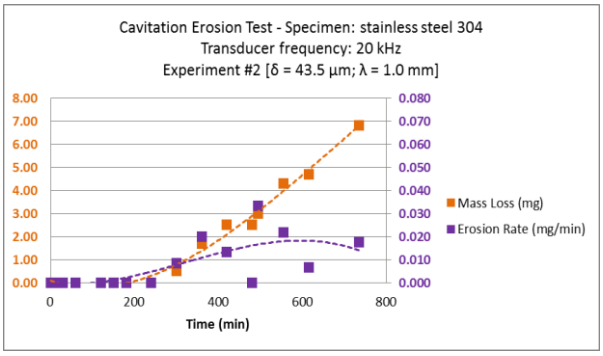

Fig. 8. Mass loss associated with experiment #2

Figure 9 shows aspects of the specimen's surface before and after being exposed to erosion.

Fig. 9. Surface aspect of Stainless steel 304, before and after exposure to erosion

4.3 Correlating cavitation with erosion resistance

Figures 10 and 11 relate the erosion rate and the average of the cavitation level for each one of the discrete intervals associated with experiments #1 and #2, respectively.

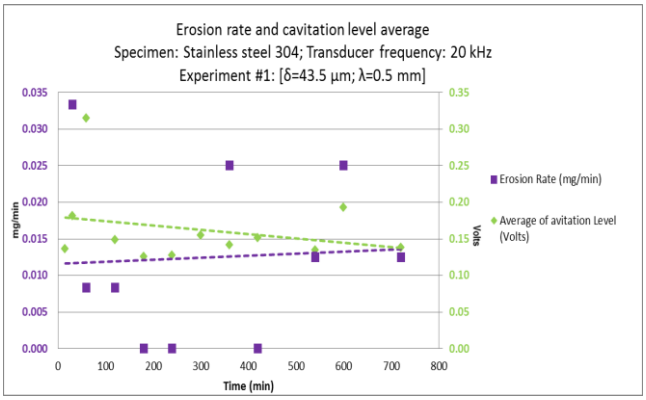

Fig.10. Erosion rate and cavitation average at experiment #1

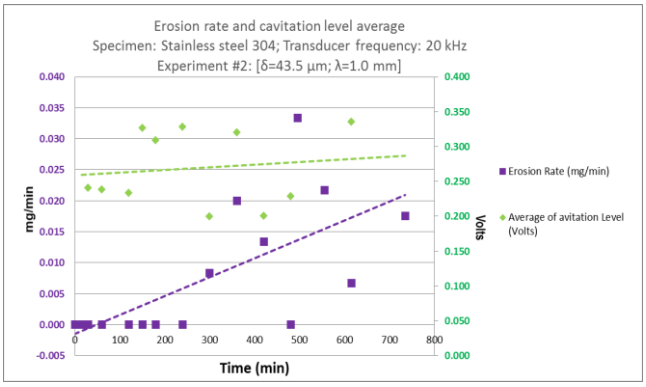

Fig.11. Erosion rate and cavitation average at experiment #2

Even though the average measurement results exposed in Figures 10 and 11 may suggest that the presence of the eroded surface may not affect the amplitude of the cavitation level, the Chi-square statistical treatment of instantaneous measurements reported in Figures 5 and 6 indicate the existence of non-uniform distributions of the cavitation level. These non-uniform distributions may be attributed to the effect of the eroded specimen in the cavitation field, by providing regions where bubbles may be held in place by radiation force from the acoustic field. These may attenuate and scatter the cavitation emissions from smaller, collapsing bubbles, and hence reduce the signal levels detected by the sensor.

5. CONCLUSIONS

The study illustrated (quantitatively) the influence of the displacement gap (λ) on the erosion and its link to cavitation phenomena. Concerning the erosion process, the specimen faced a reduction of 6.2% in mass (7.5 to 6.8 mg) when the separation between transducer and sample surface increased from λ = 0.5 mm to λ = 1.0 mm, confirming, over a similar timescale, the expected assumption that the higher the erosion rate the higher the mass loss. For the same variation of the displacement gap, the variation associated with measurement of the cavitation level exhibit a maximum variation of 2.6% (λ=0.5 mm) and 3.8% (λ=1.0 mm).

The study suggests that the presence of the eroded specimen in the cavitation field could be the cause for the existence of non-uniform distributions of the cavitation level. Further on-going experiments involving the combination of several engineering materials (therefore offering different resistance to erosion) shall shed light to establish a more comprehensive understanding of the complex mechanisms that correlates the inertial acoustic cavitation emissions with material erosion resistance.

REFERENCES

[1] M. Hodnett, Measuring Cavitation in Ultrasonic Cleaners and Processors. U.K.: National Physical Laboratory 2011.

[2] J. Santa, et al. Cavitation erosion of martensitic and austenitic stainless steel welded coatings. Wear, v. 271, n. 9-10, p. 1445-1453, JUL 29 2011 2011. ISSN 0043-1648.

[3] B. Mann, Water Droplet and Cavitation Erosion Behavior of Laser-Treated Stainless Steel and Titanium Alloy: Their Similarities. Journal of Materials Engineering and Performance, v. 22, n. 12, p. 3647-3656, DEC 2013 2013. ISSN 1059-9495.

[4] J. T. Tiong, Sonochemical and ultrasonic output analyses on dental endonosonic instruments, 2012. 299 (PhD Thesis). Chemistry, University of Bath, UK.

[5] D. C. King, Sonochemical analysis of the output of ultrasonic dental descalers, 2010. 156 (PhD Thesis). Chemistry, University of Bath, UK

[6] I. Ibanez, MSc Dissertation, Measurement and influence of cavitation induced by ultrasonic on erosion of engineering materials (in Portuguese), Postgraduate Programme in Metrology (PósMQI), Rio de Janeiro, RJ, BRAZIL, 2014.

[7] ASTM, Standard Test Method for Cavitation Erosion Using Vibratory Apparatus: 20 p. ASTM G32, 2010.

[8] B. Zeqiri, et al. A novel sensor for monitoring acoustic cavitation. Part I: Concept, theory, and prototype development. Ieee Transactions on Ultrasonics Ferroelectrics and Frequency Control, v. 50, n. 10, p. 1342-1350, OCT 2003 2003. ISSN 0885-3010.

[9] F. R. Young, 1989. Cavitation, McGraw-Hill.

[10] M. Hodnett, Calibrating cavitation sensors UIA Symposium. Washingtong D.C., USA 2015.

[11] M. Hodnett, Characterisation of industrial high power ultrasound fields using the NPL Cavitation Sensor UIA Symposium. San Diego, CA, USA 2006.

[12] M. Hodnett, B. Zeqiri, Toward a reference ultrasonic cavitation vessel: Part 2-investigating the spatial variation and acoustic pressure threshold of inertial cavitation in a 25 kHz ultrasonic field. Ieee Transactions on Ultrasonics Ferroelectrics and Frequency Control, v. 55, n. 8, p. 1809-1822, AUGUST 2008. ISSN 0885-3010.